

A Deep State-Space Model Compression Method using Upper Bound on Output Error

Hiroki Sakamoto and Kazuhiro Sato

Abstract—We study deep state-space models (Deep SSMs) that contain linear-quadratic-output (LQO) systems as internal blocks and present a compression method with a provable output error guarantee. We first derive an upper bound on the output error between two Deep SSMs and show that the bound can be expressed via the h^2 -error norms between the layerwise LQO systems, thereby providing a theoretical justification for existing model order reduction (MOR)-based compression. Building on this bound, we formulate an optimization problem in terms of the h^2 -error norm and develop a gradient-based MOR method. On the IMDb task from the Long Range Arena benchmark, we demonstrate that our compression method achieves strong performance. Moreover, unlike prior approaches, we reduce roughly 80% of trainable parameters without retraining, with only a 4–5% performance drop.

Index Terms—Model compression; Deep State-Space Models; Optimal h^2 Model Order Reduction; Linear Quadratic Output systems

I. INTRODUCTION

Deep state-space models (Deep SSMs) [1]–[5] are deep models that incorporate linear state-space models into intermediate layers, and they have attracted attention as sequence models that can efficiently handle long-range dependencies and nonlinearities. As representative examples, S5 [4] and Mamba [5] achieve state-of-the-art performance on various tasks in the Long Range Arena (LRA) benchmark [6] without using the attention mechanism employed in Transformers [7], and their effectiveness has been reported on real-world data [8]. In theory, Deep SSMs combined with simple nonlinear layers have been shown to possess Transformer-comparable capabilities in dynamic token selection and certain nonparametric regression settings [9]. Achieving high performance often requires a sufficient number of parameters; in particular, for Deep SSMs, one can build high-performance models by enlarging the parameter size of the embedded linear state-space models.

When deploying trained models to a variety of tasks, it is desirable to obtain compact models with fewer parameters while maintaining the performance of large models. To construct small-scale Deep SSMs, one may apply general model-compression techniques developed for deep learning models. Well-known approaches include pruning, quantization, and knowledge distillation, which are effective also for compressing Deep SSMs [10]. On the other hand, it has recently been recognized that model order reduction (MOR), a classical topic

H. Sakamoto and K. Sato are with the Department of Mathematical Informatics, Graduate School of Information Science and Technology, The University of Tokyo, Tokyo 113-8656, Japan, email: soccer-books0329@g.ecc.u-tokyo.ac.jp (H. Sakamoto), kazuhiro@mist.i.u-tokyo.ac.jp (K. Sato)

in systems and control theory, is effective as a compression method for Deep SSMs [11]–[14].

MOR-based compression seeks to reduce the number of parameters of the linear state-space models placed within Deep SSMs while preserving the performance of the original large model. [11] applied Balanced Truncation (BT) to the linear state-space model at each layer and used the results as initialization for retraining to construct accurate compressed models. [12] also used BT as in [11], but added a regularization term to the training objective to reduce the nonzero eigenvalues of the matrix A , thereby constructing a one-shot compressed model. Furthermore, [14] proposed a method that constructs reduced models that are optimal in the \mathcal{H}^2 -norm sense while preserving properties specific to Deep SSMs; using these as initialization for retraining yields compressed models that outperform BT-based methods [11]. In addition, [13] introduced an \mathcal{H}^∞ -based indicator (the \mathcal{H}^∞ score) to efficiently eliminate modes within the linear state-space models.

As shown in Fig. 1, in these existing studies, compression is performed by applying MOR individually to each linear state-space model placed at intermediate layers, based on various indicators and training schemes. While this approach constructs reduced models that approximate the input-output behavior of each individual linear state-space model, it can fail to sufficiently approximate the final output of the original Deep SSM as a whole.

In this work, to adequately approximate the overall performance of the original Deep SSM, we construct reduced models that reflect inter-layer interactions (see Fig. 1). In particular, to the best of our knowledge, this is the first study—from the viewpoint of systems and control theory—to propose a compression method that directly guarantees the overall output performance of a Deep SSM. To facilitate theoretical analysis based on MOR theory [15]–[17], we consider S5 [4] (with a quadratic activation function immediately after each linear state-space block) and, more generally, Deep SSMs that internally contain linear quadratic-output (LQO) systems, and we develop a compression method with a provable upper bound on the output error.

The contributions of this paper are:

- To construct a reduced Deep SSM that minimizes the output error $\|s_{\text{out}} - \hat{s}_{\text{out,pro}}\|_{\ell_L^\infty}$ for any input sequence s_{in} —and since directly optimizing this quantity is challenging—we derive an upper bound on the output error between two Deep SSMs, as illustrated in Fig. 1 (top). The derived bound shows that minimizing the h^2 error of each individual state-space model within a Deep SSM, as shown in Fig. 1 (bottom), leads to minimizing an upper bound of the overall output error.

Although the internal state-space models of the Deep SSMs and the activation functions we consider differ from prior work, this result implies that the bound provides a theoretical justification for existing MOR methods [11], [14]. Finally, we introduce an optimization algorithm with a stationary point guarantee that minimizes the bound while preserving the unique properties of Deep SSMs.

- We show numerically that the proposed method yields accurate compressed models. Unlike [11], [14], we report that the proposed method can sometimes outperform HiPPO-based training [1] without retraining. Moreover, for the retraining-free compression methods [13], when comparing accuracy at the same state dimension (cf. [13, Fig.2]), the proposed method—despite differences in the Deep SSM architecture—constructed compressed models with superior performance. This provides a practical contribution: it enables low-cost, high-performance deployment in settings where retraining is impractical or impossible—e.g., under strict compute constraints.

The paper is organized as follows. Section II introduces discrete-time complex LQO systems. Section III presents Deep SSMs that include them and our compression strategy. Using the output error bound from Section IV, Section V formulates the MOR problem and proposes an optimization algorithm. Section VI reports experiments, and Section VII concludes.

Notation: For vectors, $\|\cdot\|$ denotes the Euclidean norm and $\|\cdot\|_\infty$ denotes the infinity norm. For matrices, $\|\cdot\|_2$ denotes the operator (spectral) norm and $\|\cdot\|$ denotes the Frobenius norm. Let $(X, \|\cdot\|)$ be a normed vector space (e.g., $X = \mathbb{R}^m$ or \mathbb{C}^m with the Euclidean norm) and define, for $1 \leq p \leq \infty$, $\ell^p(X) := \left\{ x = (x_k)_{k \geq 0} \in X \mid \sum_{k \geq 0} \|x_k\|^p < \infty \right\}$, and $\ell^\infty(X) := \left\{ x = (x_k)_{k \geq 0} \in X \mid \sup_{k \geq 0} \|x_k\| < \infty \right\}$. Throughout, we write $\ell^p := \ell^p(X)$ for $1 \leq p \leq \infty$. For $x \in \ell^p$, define $\|x\|_{\ell^p} := (\sum_{k \geq 0} \|x_k\|^p)^{1/p}$ for $1 \leq p < \infty$; for a finite horizon L , define $\|x\|_{\ell_L^p} := (\sum_{k=0}^{L-1} \|x_k\|^p)^{1/p}$ for $1 \leq p < \infty$ and $\|x\|_{\ell_L^\infty} := \max_{0 \leq k \leq L-1} \|x_k\|$.

The conjugate transpose is $(\cdot)^*$ (so $A = A^*$ means Hermitian; for real matrices, symmetric), and $(\cdot)^\top$ denotes transpose. For a matrix X , $\text{vec}(X)$ stacks its columns into a single vector. The symbol \otimes denotes the Kronecker product, and \odot denotes the elementwise (Hadamard) product.

For a real-valued function f , $\text{d}f$ denotes its (total) differential; for a perturbation $\text{d}\theta$ of θ , we write $\text{d}f = \langle \nabla_\theta f, \text{d}\theta \rangle$, where the inner product is $\langle A, B \rangle := \text{Re}(\text{tr}(A^* B))$. For multiple variables $\theta = (\theta_1, \theta_2, \dots)$, we write $\text{d}f = \sum_j \langle \nabla_{\theta_j} f, \text{d}\theta_j \rangle$.

The symbol $*$ denotes discrete-time convolution, defined for $k \geq 0$ by $(x * h)[k] := \sum_{m=0}^k x[m]h[k-m]$. For $1 \leq p, q, r \leq \infty$ satisfying $\frac{1}{p} + \frac{1}{q} = 1 + \frac{1}{r}$, $x \in \ell^p$ and $h \in \ell^q$ obey the Young's convolution inequality

$$\|x * h\|_{\ell^r} \leq \|x\|_{\ell^p} \|h\|_{\ell^q}.$$

In addition, for the finite-horizon norms ℓ_L^p , the same bounds hold.

II. DISCRETE-TIME COMPLEX LQO SYSTEMS

In this section, we describe the general properties of the state-space models that constitute the Deep SSM considered

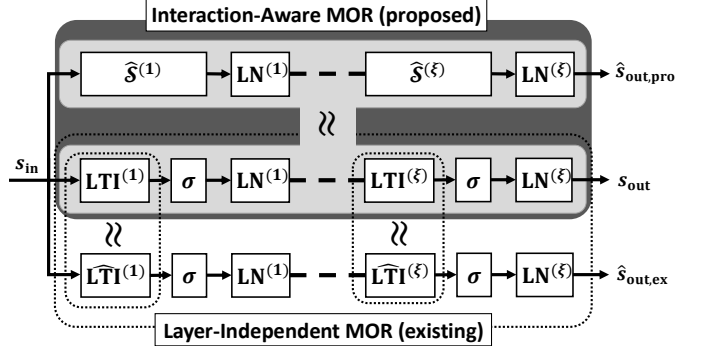


Fig. 1. Comparison between existing MOR methods and the proposed method for ξ -layer Deep SSMs. Existing methods perform MOR independently on the linear time-invariant (LTI) subsystems within a Deep SSM and produce $\hat{s}_{\text{out},\text{ex}}$. In contrast, the proposed method constructs a reduced Deep SSM with reduced LQO systems $\{\hat{S}^{(i)}\}_{i=1}^\xi$ that approximates the pretrained Deep SSM's output s_{out} while accounting for inter-layer interactions, the nonlinearity σ , and LayerNorm (LN); in particular, it minimizes $\|s_{\text{out}} - \hat{s}_{\text{out},\text{pro}}\|_{\ell_L^\infty}$ for a given input sequence s_{in} .

in this study. Specifically, we consider the following discrete-time complex LQO system:

$$\mathcal{S} : \begin{cases} x_k = Ax_{k-1} + Bu_k, \\ y_k = Cx_k + M(x_k \otimes x_k), \end{cases} \quad (1)$$

where $u_k \in \mathbb{C}^m$, $x_k \in \mathbb{C}^n$, $y_k \in \mathbb{C}^p$, and $A \in \mathbb{C}^{n \times n}$, $B \in \mathbb{C}^{n \times m}$, $C \in \mathbb{C}^{p \times n}$, $M = [\text{vec}(M_1), \dots, \text{vec}(M_p)]^\top \in \mathbb{C}^{p \times n^2}$. For any $i = 1, \dots, p$, let $U_i \in \mathbb{C}^{c \times n}$ and $M_i = U_i^* U_i \in \mathbb{C}^{n \times n}$ be Hermitian. We assume that A is (discrete-time) stable, i.e., all its eigenvalues lie strictly inside the open unit disk.

The Volterra kernels of (1) are

$$h_1[t] = CA^t B, \quad h_2[t_1, t_2] = M(A^{t_1} B \otimes A^{t_2} B),$$

and, with $x_{-1} = 0$, (1) is equivalent to the convolution representation

$$y_k = \sum_{t=0}^k h_1[t] \cdot u_{k-t} + \sum_{t_1=0}^k \sum_{t_2=0}^k h_2[t_1, t_2] \cdot (u_{k-t_1} \otimes u_{k-t_2}). \quad (2)$$

The h^2 -norm of (1) is defined by

$$\|\mathcal{S}\|_{h^2}^2 := \|h_1\|_{\ell^2}^2 + \|h_2\|_{\ell^2}^2.$$

In particular, on the finite horizon $\{0, 1, \dots, L-1\}$, the h_L^2 -norm is

$$\|\mathcal{S}\|_{h_L^2}^2 := \|h_1\|_{\ell_L^2}^2 + \|h_2\|_{\ell_L^2}^2.$$

Since (1) is asymptotically stable, letting P_L be the solution of the finite-horizon Lyapunov equation

$$P_L = AP_L A^* + BB^* - A^L BB^* (A^*)^L,$$

we can write

$$\|h_1\|_{\ell_L^2}^2 = \text{tr}(CP_L C^*), \quad \|h_2\|_{\ell_L^2}^2 = \sum_{k=1}^p \text{tr}(P_L M_k P_L M_k^*),$$

see [16], [17] for details.

A reduced-order model (ROM) for (1) is given by

$$\hat{\mathcal{S}} : \begin{cases} \hat{x}_k = \hat{A}\hat{x}_{k-1} + \hat{B}u_k, \\ \hat{y}_k = \hat{C}\hat{x}_k + \hat{M}(\hat{x}_k \otimes \hat{x}_k), \end{cases} \quad (3)$$

where $u_k \in \mathbb{C}^m$, $\hat{x}_k \in \mathbb{C}^r$, $\hat{y}_k \in \mathbb{C}^p$, $\hat{A} \in \mathbb{C}^{r \times r}$, $\hat{B} \in \mathbb{C}^{r \times m}$, $\hat{C} \in \mathbb{C}^{p \times r}$, $\hat{M} = [\text{vec}(\hat{M}_1), \dots, \text{vec}(\hat{M}_p)]^\top \in \mathbb{C}^{p \times r^2}$, with \hat{A} stable and each $\hat{M}_i \in \mathbb{C}^{r \times r}$ Hermitian.

For the same input u_k , an output error inequality between (1) and (3) holds [15]:

$$\begin{aligned} & \|y - \hat{y}\|_{\ell_L^\infty}^2 \\ & \leq (\|h_1 - \hat{h}_1\|_{\ell_L^2}^2 + \|h_2 - \hat{h}_2\|_{\ell_L^2}^2)(1 + \|u\|_{\ell_L^2}^2)\|u\|_{\ell_L^2}^2 \\ & = \|\mathcal{S} - \hat{\mathcal{S}}\|_{h_L^2}^2(1 + \|u\|_{\ell_L^2}^2)\|u\|_{\ell_L^2}^2. \end{aligned} \quad (4)$$

Let \tilde{P}_L and \hat{P}_L be the solutions to the finite-horizon Sylvester/Lyapunov equations

$$\tilde{P}_L = A\tilde{P}_L\hat{A}^* + B\hat{B}^* - A^L B\hat{B}^*(\hat{A}^*)^L, \quad (5)$$

$$\hat{P}_L = \hat{A}\hat{P}_L\hat{A}^* + \hat{B}\hat{B}^* - \hat{A}^L\hat{B}\hat{B}^*(\hat{A}^*)^L. \quad (6)$$

Then the squared h_L^2 error norm satisfies

$$\begin{aligned} \|\mathcal{S} - \hat{\mathcal{S}}\|_{h_L^2}^2 &= \text{tr}(C\tilde{P}_L C^*) + \text{tr}(\hat{C}\hat{P}_L\hat{C}^*) - 2\text{Re}\text{tr}(C\tilde{P}_L\hat{C}^*) \\ &+ \sum_{k=1}^p \left(\text{tr}(P_L M_k P_L M_k) + \text{tr}(\hat{P}_L \hat{M}_k \hat{P}_L \hat{M}_k) \right. \\ &\quad \left. - 2\text{Re}\text{tr}(\tilde{P}_L^* M_k \tilde{P}_L \hat{M}_k) \right). \end{aligned} \quad (7)$$

From (4), for any sufficiently small input norm, making the h_L^2 error (7) small guarantees a sufficiently small output error. We note that directly optimizing the left-hand side of (4) is difficult.

III. PROBLEM SETTING

A. Deep SSMs with Linear Quadratic-Output Systems

In this work, we consider a ξ -layer Deep SSM with the structure shown in Fig. 2. At the input layer, an input sequence $(s_k)_{k=0}^{L-1}$ with feature dimension H is given and transformed into the m -dimensional input of the first intermediate layer, $s_{\text{in},k} = u_k^{(1)} \in \mathbb{R}^m$. For a general i -th intermediate layer ($i = 1, 2, \dots, \xi$), the input $u_k^{(i)}$ is mapped to the output $y_k^{(i)}$ by the following complex LQO system corresponding to (1):

$$\mathcal{S}^{(i)} : \begin{cases} x_k^{(i)} = A^{(i)}x_{k-1}^{(i)} + B^{(i)}u_k^{(i)}, \\ y_k^{(i)} = C^{(i)}x_k^{(i)} + M^{(i)}(x_k^{(i)} \otimes x_k^{(i)}), \end{cases} \quad (8)$$

where $u_k^{(i)} \in \mathbb{R}^m$, $x_k^{(i)} \in \mathbb{C}^n$, $y_k^{(i)} \in \mathbb{C}^m$, $A^{(i)} \in \mathbb{C}^{n \times n}$ is diagonal and (discrete-time) stable, $B^{(i)} \in \mathbb{C}^{n \times m}$, $C^{(i)} \in \mathbb{C}^{m \times n}$, $M^{(i)} \in \mathbb{C}^{m \times n^2}$, and for any $j = 1, \dots, m$, $U_j^{(i)} \in \mathbb{C}^{c \times n}$ with $M_j^{(i)} = (U_j^{(i)})^* U_j^{(i)} \in \mathbb{C}^{n \times n}$ Hermitian. For stable training, we apply a residual connection to the real parts of the input $u_k^{(i)}$ and the output $y_k^{(i)}$, followed by layer normalization (LN):

$$z_k^{(i)} = u_k^{(i)} + \text{Re}(y_k^{(i)}), \quad (9)$$

$$u_k^{(i+1)} = \text{LN}_{\gamma_1^{(i)}, \gamma_2^{(i)}}(z_k^{(i)}), \quad (10)$$

where, for $\varepsilon > 0$, LN is defined by

$$\text{LN}_{\gamma_1^{(i)}, \gamma_2^{(i)}}(z_k^{(i)}) = \gamma_1^{(i)} \odot \frac{z_k^{(i)} - \mu_{k,i}}{\sigma_{k,i}} + \gamma_2^{(i)}, \quad (11)$$

$$\mu_{k,i} := \frac{1}{m} \mathbf{1}^\top z_k^{(i)}, \quad \sigma_{k,i} := \sqrt{\frac{1}{m} \|z_k^{(i)} - \mu_{k,i}\mathbf{1}\|^2 + \varepsilon}.$$

Note that $\gamma_1^{(i)}$ and $\gamma_2^{(i)}$ are the learnable affine parameters of LN at layer i , representing the per-feature scale and bias, respectively. The sequence $(s_{\text{out},k})_{k=0}^{L-1} := (u_k^{(\xi+1)})_{k=0}^{L-1}$ obtained in this manner is the final output of the intermediate layers of the Deep SSM. The sequence $(s_{\text{out},k})_{k=0}^{L-1}$ is then mapped by an output layer to an output of the desired shape.

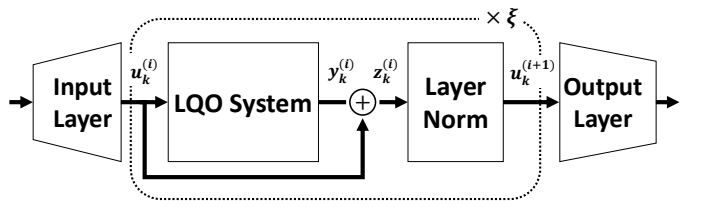


Fig. 2. Structure of the Deep SSM considered in this work.

Remark 1. The Deep SSM used in this study can be interpreted as a generalization of S5 [4] when the activation immediately after each linear state-space block is the quadratic function $\sigma(x) = (|x_1|^2, \dots, |x_m|^2) \in \mathbb{R}^m$. In S5, the input-output relation from u_k to y_k is expressed as

$$\begin{cases} x_k = A_{S5} x_{k-1} + B_{S5} u_k, \\ y_k = \sigma(C_{S5} x_k). \end{cases}$$

This coincides with (8) in the case $A = A_{S5}$, $B = B_{S5}$, $C = 0$, and $M_j = C_{S5,j}^* C_{S5,j}$, where $C_{S5,j}$ denotes the j -th row of C_{S5} . In this work, we model the input-output relation from u_k to y_k in Deep SSMs using more general C and M matrices.

B. MOR-Based Compression of Deep SSMs

The MOR-based compression of Deep SSMs [11], [14] constructs a reduced Deep SSM (compressed model) via the following procedure:

- 1) Initialize the parameters of the Deep SSM via the HiPPO initialization framework [1] and pretrain the model.
- 2) Apply MOR to the linear state-space models embedded in the pretrained Deep SSM.
- 3) Use the reduced models obtained by MOR as initialization and retrain.

It is known that using the MOR-based reduced models as initialization for retraining yields high-performance reduced Deep SSMs compared with random initialization or HiPPO initialization [11], [14]. In [11], [14], the linear state-space models placed at each layer are treated independently, and reduced models that approximate the linear state-space model of each layer are constructed. While this may reduce each layerwise output error $y^{(i)} - \hat{y}^{(i)}$, it does not account for inter-layer interactions; consequently, the reduced Deep SSM output \hat{s}_{out} may fail to sufficiently approximate the original

output s_{out} . Therefore, in order to obtain a high-performance reduced Deep SSM after retraining, it is desirable to construct a good initial reduced Deep SSM that sufficiently approximates $s_{\text{out}} - \hat{s}_{\text{out}}$.

In this work, for an input sequence $(s_{\text{in},k})_{k=0}^{L-1}$ of length L , we construct a reduced Deep SSM that approximates the final intermediate output $(s_{\text{out},k})_{k=0}^{L-1}$ of a ξ -layer Deep SSM. Here, we call the pretrained model whose layers are composed of n -dimensional complex LQO systems (1) an n -dimensional Deep SSM, and we call the model in which the i -th layer is given by the reduced model (3) with $r = r_i$ an r_i -dimensional Deep SSM. In particular, unlike prior MOR-based approaches for Deep SSMs [11]–[14], our goal is to construct an r_i -dimensional Deep SSM that directly reduces $\|s_{\text{out}} - \hat{s}_{\text{out}}\|_{\ell_L^\infty}$ for any input sequence s_{in} (see Fig. 1). We note that directly optimizing $\|s_{\text{out}} - \hat{s}_{\text{out}}\|_{\ell_L^\infty}$ is difficult due to the complexity of the function. For details, please refer to Remark 3 in Section V.

IV. OUTPUT ERROR ANALYSIS FOR DEEP SSMs

For any input sequence $(s_{\text{in},k})_{k=0}^{L-1}$, we aim to construct a reduced Deep SSM that minimizes the output error

$$e_\xi := \|s_{\text{out}} - \hat{s}_{\text{out}}\|_{\ell_L^\infty} \quad (12)$$

of Deep SSMs, and derive an upper bound on e_ξ that depends on the input. Hereafter, for the i -th intermediate layer of the n -dimensional Deep SSM and the r_i -dimensional Deep SSM, denote their LQO inputs/outputs by $(u_k^{(i)}, y_k^{(i)})$ and $(\hat{u}_k^{(i)}, \hat{y}_k^{(i)})$, respectively, for all k , and assume $u_k^{(1)} = \hat{u}_k^{(1)}$.

Lemma 1. *Let $u = (u_k)_{k=0}^{L-1} \in \ell_L^2$. Then, the following inequality holds:*

$$\|u \otimes u - \hat{u} \otimes \hat{u}\|_{\ell_L^2} \leq \|u - \hat{u}\|_{\ell_L^2} (\|u\|_{\ell_L^2} + \|\hat{u}\|_{\ell_L^2}). \quad (13)$$

Proof. See Appendix. \square

Theorem 1. *Let $\mathcal{S}^{(i)} = (A^{(i)}, B^{(i)}, C^{(i)}, M^{(i)})$ denote the n -dimensional state-space model at the i -th layer of the Deep SSM in (8), and let $\hat{\mathcal{S}}^{(i)} = (\hat{A}^{(i)}, \hat{B}^{(i)}, \hat{C}^{(i)}, \hat{M}^{(i)})$ denote the $r = r_i$ -dimensional state-space model at the i -th layer of the r_i -dimensional Deep SSM. Assume $\mathcal{S}^{(i)}$ and $\hat{\mathcal{S}}^{(i)}$ are asymptotically stable for all $i = 1, 2, \dots, \xi$. Then*

$$\begin{aligned} e_\xi &\leq \sum_{i=1}^{\xi} G_i \|\mathcal{S}^{(i)} - \hat{\mathcal{S}}^{(i)}\|_{\ell_L^2} \\ &\quad \cdot \left(\|\hat{u}^{(i)}\|_{\ell_L^2} \sqrt{1 + \|\hat{u}^{(i)}\|_{\ell_L^2}^2} \right), \end{aligned} \quad (14)$$

where, with $\omega := \max_i (\text{Lip}(\text{LN}_{\gamma_1^{(i)}, \gamma_2^{(i)}}))$ denoting the maximum Lipschitz constant of LN (11),

$$\begin{aligned} G_i &= \omega^{\xi-i+1} \left(\prod_{j=i+1}^{\xi} g_j \right), \\ g_j &= 1 + \sqrt{L} \cdot \left\{ \|h_1^{(j)}\|_{\ell_L^2} + \|h_2^{(j)}\|_{\ell_L^2} (\|u^{(j)}\|_{\ell_L^2} + \|\hat{u}^{(j)}\|_{\ell_L^2}) \right\}. \end{aligned}$$

Proof. First, for the two LQO systems $\mathcal{S}^{(i)}$ and $\hat{\mathcal{S}}^{(i)}$ at layer i , let $e_{\text{SSM},i} := \|y^{(i)} - \hat{y}^{(i)}\|_{\ell_L^\infty}$ denote the output error. From (2),

$$\begin{aligned} &y_k^{(i)} - \hat{y}_k^{(i)} \\ &= \sum_{\ell=0}^k h_1^{(i)}[\ell] \cdot u_{k-\ell}^{(i)} - \hat{h}_1^{(i)}[\ell] \cdot \hat{u}_{k-\ell}^{(i)} \\ &\quad + \sum_{\ell_1=0}^k \sum_{\ell_2=0}^k h_2^{(i)}[\ell_1, \ell_2] \cdot (u_{k-\ell_1}^{(i)} \otimes u_{k-\ell_2}^{(i)}) \\ &\quad - \hat{h}_2^{(i)}[\ell_1, \ell_2] \cdot (\hat{u}_{k-\ell_1}^{(i)} \otimes \hat{u}_{k-\ell_2}^{(i)}) \\ &= \sum_{\ell=0}^k h_1^{(i)}[\ell] \cdot (u_{k-\ell}^{(i)} - \hat{u}_{k-\ell}^{(i)}) + (h_1^{(i)}[\ell] - \hat{h}_1^{(i)}[\ell]) \cdot \hat{u}_{k-\ell}^{(i)} \\ &\quad + \sum_{\ell_1=0}^k \sum_{\ell_2=0}^k h_2^{(i)}[\ell_1, \ell_2] \cdot (u_{k-\ell_1}^{(i)} \otimes u_{k-\ell_2}^{(i)} \\ &\quad - \hat{u}_{k-\ell_1}^{(i)} \otimes \hat{u}_{k-\ell_2}^{(i)}) \\ &\quad + (h_2^{(i)}[\ell_1, \ell_2] - \hat{h}_2^{(i)}[\ell_1, \ell_2]) \cdot (\hat{u}_{k-\ell_1}^{(i)} \otimes \hat{u}_{k-\ell_2}^{(i)}). \end{aligned}$$

Hence, by the triangle inequality,

$$\begin{aligned} e_{\text{SSM},i} &\leq \|h_1^{(i)} * (u^{(i)} - \hat{u}^{(i)})\|_{\ell_L^\infty} + \|(h_1^{(i)} - \hat{h}_1^{(i)}) * \hat{u}^{(i)}\|_{\ell_L^\infty} \\ &\quad + \|h_2^{(i)} * (u^{(i)} \otimes u^{(i)} - \hat{u}^{(i)} \otimes \hat{u}^{(i)})\|_{\ell_L^\infty} \\ &\quad + \|(h_2^{(i)} - \hat{h}_2^{(i)}) * (\hat{u}^{(i)} \otimes \hat{u}^{(i)})\|_{\ell_L^\infty}. \end{aligned}$$

Let $\alpha_{1,i} := \|h_1^{(i)}\|_{\ell_L^2}$, $\alpha_{2,i} := \|h_2^{(i)}\|_{\ell_L^2}$, $\tilde{\alpha}_{1,i} := \|h_1^{(i)} - \hat{h}_1^{(i)}\|_{\ell_L^2}$, $\tilde{\alpha}_{2,i} := \|h_2^{(i)} - \hat{h}_2^{(i)}\|_{\ell_L^2}$, $\beta_i := \|u^{(i)}\|_{\ell_L^2}$, and $\hat{\beta}_i := \|\hat{u}^{(i)}\|_{\ell_L^2}$. By Young's convolution inequality and the relation $\|\cdot\|_{\ell_L^2} \leq \sqrt{L} \|\cdot\|_{\ell_L^\infty}$,

$$\begin{aligned} \|h_1^{(i)} * (u^{(i)} - \hat{u}^{(i)})\|_{\ell_L^\infty} &\leq \sqrt{L} \cdot \alpha_{1,i} \cdot e_{i-1} \\ \|(h_1^{(i)} - \hat{h}_1^{(i)}) * \hat{u}^{(i)}\|_{\ell_L^\infty} &\leq \tilde{\alpha}_{1,i} \cdot \hat{\beta}_i. \end{aligned}$$

Also, by Lemma 1, we get

$$\begin{aligned} &\|h_2^{(i)} * (u^{(i)} \otimes u^{(i)} - \hat{u}^{(i)} \otimes \hat{u}^{(i)})\|_{\ell_L^\infty} \\ &\leq \alpha_{2,i} \cdot \|u^{(i)} \otimes u^{(i)} - \hat{u}^{(i)} \otimes \hat{u}^{(i)}\|_{\ell_L^2} \\ &\leq \sqrt{L} \cdot \alpha_{2,i} \cdot e_{i-1} \cdot (\beta_i + \hat{\beta}_i), \end{aligned}$$

and

$$\begin{aligned} \|(h_2^{(i)} - \hat{h}_2^{(i)}) * (\hat{u}^{(i)} \otimes \hat{u}^{(i)})\|_{\ell_L^\infty} &\leq \tilde{\alpha}_{2,i} \cdot \|\hat{u}^{(i)} \otimes \hat{u}^{(i)}\|_{\ell_L^2} \\ &= \tilde{\alpha}_{2,i} \cdot \hat{\beta}_i^2. \end{aligned}$$

Thus, with $\kappa_i := \sqrt{L} \cdot (\alpha_{1,i} + \alpha_{2,i}(\beta_i + \hat{\beta}_i))$,

$$\begin{aligned} e_{\text{SSM},i} &\leq \kappa_i e_{i-1} + \tilde{\alpha}_{1,i} \hat{\beta}_i + \tilde{\alpha}_{2,i} \hat{\beta}_i^2 \\ &\leq \kappa_i e_{i-1} + \sqrt{\tilde{\alpha}_{1,i}^2 + \tilde{\alpha}_{2,i}^2} \sqrt{1 + \hat{\beta}_i^2} \hat{\beta}_i. \end{aligned}$$

Taking the residual connection (9) and LN (10) into account, we obtain the recurrence for the output error e_i :

$$\begin{aligned} e_i &\leq \text{Lip}(\text{LN}_{\gamma_1^{(i)}, \gamma_2^{(i)}}) \|z^{(i)} - \hat{z}^{(i)}\|_{\ell_L^\infty} \\ &\leq \text{Lip}(\text{LN}_{\gamma_1^{(i)}, \gamma_2^{(i)}}) (e_{\text{SSM},i} + e_{i-1}) \\ &\leq \text{Lip}(\text{LN}_{\gamma_1^{(i)}, \gamma_2^{(i)}}) \\ &\quad \cdot \left\{ (1 + \kappa_i) e_{i-1} + \sqrt{\tilde{\alpha}_{1,i}^2 + \tilde{\alpha}_{2,i}^2} \cdot \sqrt{1 + \hat{\beta}_i^2} \cdot \hat{\beta}_i \right\}. \end{aligned} \quad (15)$$

Using the relation $\|\mathcal{S}^{(i)} - \hat{\mathcal{S}}^{(i)}\|_{h_L^2} = (\tilde{\alpha}_{1,i}^2 + \tilde{\alpha}_{2,i}^2)^{1/2}$ and solving the recurrence (15) with $\beta_i = \hat{\beta}_i$ and $e_0 = 0$, we obtain the global bound (14). \square

In the Deep SSM considered here, the outputs of the state-space blocks are normalized by (11), so the inputs $\|u^{(j)}\|_{\ell_L^2}$ and $\|\hat{u}^{(j)}\|_{\ell_L^2}$ at layer j can be regarded as bounded by a constant. Thus, we have the following corollary.

Corollary 1. *Let b be a constant and assume $\max_{1 \leq j \leq \xi} (\|u^{(j)}\|_{\ell_L^2}, \|\hat{u}^{(j)}\|_{\ell_L^2}) \leq b$. Under the assumptions of Theorem 1,*

$$e_\xi \leq (b\sqrt{1+b^2}) \sum_{i=1}^{\xi} \tilde{G}_i \|\mathcal{S}^{(i)} - \hat{\mathcal{S}}^{(i)}\|_{h_L^2}, \quad (16)$$

where

$$\begin{aligned} \tilde{G}_i &= \omega^{\xi-i+1} \left(\prod_{j=i+1}^{\xi} \tilde{g}_j \right), \\ \tilde{g}_j &= 1 + \sqrt{L} \left(\|h_1^{(j)}\|_{\ell_L^2} + 2b \|h_2^{(j)}\|_{\ell_L^2} \right). \end{aligned}$$

Proof. By Theorem 1, it can be shown. \square

From (16), it can be seen that the h^2 errors of the two LQO systems deployed in each layer affect the output error. This result provides a theoretical justification for existing ad hoc MOR methods [11], [14]. In particular, under sufficiently small input norms, reducing the h^2 errors of the two systems can minimize the overall output error e_ξ of the Deep SSM.

Lemma 2. *Let $m \geq 2$ and $\varepsilon > 0$. Denote by $\text{Lip}(\text{LN}_{\gamma_1, \gamma_2})$ the Lipschitz constant of LN in (11). Then, for $\gamma_1, \gamma_2 \in \mathbb{R}^m$,*

$$\frac{\|\gamma_1\|_\infty}{\sqrt{\varepsilon}} \sqrt{1 - \frac{1}{m}} \leq \text{Lip}(\text{LN}_{\gamma_1, \gamma_2}) \leq \frac{\|\gamma_1\|_\infty}{\sqrt{\varepsilon}}.$$

Proof. See Appendix. \square

Remark 2. *By Lemma 2, taking ε sufficiently small yields $\text{Lip}(\text{LN}_{\gamma_1, \gamma_2}) \gg 1$. Moreover, $\tilde{g}_j \geq 1$ for any j . Therefore, by Corollary 1, for any i , we obtain $\tilde{G}_i \geq \tilde{G}_{i+1}$. This means that h_L^2 -norm errors in shallower layers have a stronger effect on the final intermediate output error of the Deep SSM.*

V. MODEL REDUCTION FOR DEEP SSM

A. Model Order Reduction Problem

Based on Corollary 1, we formulate the MOR problem. In particular, we consider the optimization problem that minimizes the upper bound in (16). Let $\hat{U}^{(i)} = [\text{vec}(\hat{U}_1^{(i)}), \dots, \text{vec}(\hat{U}_m^{(i)})]^\top \in \mathbb{C}^{m \times cr_i}$ and define $\mathcal{C}_i := \mathbb{C}_{-}^{r_i} \times \mathbb{C}^{r_i \times m} \times \mathbb{C}^{m \times r_i} \times \mathbb{C}^{m \times cr_i}$ and $\hat{\mathbf{S}} := (\hat{\mathbf{S}}^{(i)})_{i=1}^{\xi}$. Then the MOR problem can be written as

$$\begin{aligned} \text{minimize } f(\hat{\mathbf{S}}) &:= \sum_{i=1}^{\xi} \tilde{G}_i \|\mathcal{S}^{(i)} - \hat{\mathcal{S}}^{(i)}\|_{h_L^2} \\ \text{subject to } (\hat{\Lambda}^{(i)}, \hat{B}^{(i)}, \hat{C}^{(i)}, \hat{U}^{(i)}) &\in \mathcal{C}_i, \quad \forall i = 1, \dots, \xi. \end{aligned} \quad (17)$$

Here, $\mathcal{S}^{(i)}$ and $\hat{\mathcal{S}}^{(i)}$ denote, respectively for the i -th layer of the Deep SSM, the systems (1) with $A := \text{diag}(\Lambda)$ and (3) with $\hat{A} := \text{diag}(\hat{\Lambda})$.

In the MOR problem (17), \tilde{G}_i is given independently of the optimization variables; therefore, it suffices to minimize $\|\mathcal{S}^{(i)} - \hat{\mathcal{S}}^{(i)}\|_{h_L^2}$, which is the same setting as the existing method described in Fig. 1. Note, as discussed in [14], that because the internal linear state-space models in the Deep SSM are (i) defined on a finite horizon, (ii) required to be stability-guaranteed for reliable training, and (iii) formulated over the complex field, recent \mathcal{H}^2 MOR theory for LQO systems [16], [17] is not directly applicable in some cases.

Remark 3. *In model reduction for Deep SSMs, it is preferable to optimize the objective f in (17) rather than the aggregate output error e_ξ defined in (12). The quantity e_ξ is difficult to optimize directly because it is nonsmooth and lacks a closed-form characterization, and it involves multi-fold products of layerwise Volterra kernels h_1, h_2 . In contrast, the objective f is analytic and smooth, which facilitates the design of efficient optimization algorithms; moreover, it enables the construction of ROMs that preserve Deep SSM-specific properties as in (17). Motivated by these considerations, our goal is not to minimize e_ξ directly, but to solve the optimization problem (17) so as to obtain reduced parameters that decrease e_ξ .*

B. Gradients for (17)

We derive the gradients for (17) following [17].

Lemma 3. *Let the time-limited \mathcal{H}^2 error between the complex LQO system (1) and its reduced system (3) be $\varphi(\hat{\mathbf{S}}) := \|\mathcal{S} - \hat{\mathcal{S}}\|_{h_L^2}^2$. Then the gradients of $\varphi(\hat{\mathbf{S}})$ are given by*

$$\begin{aligned} \nabla_{\hat{A}} \varphi &= 2(-(\tilde{Y}_L + 2\tilde{Z}_L)^* \tilde{P}_L + (\hat{Y}_L + 2\hat{Z}_L) \hat{P}_L + L_L), \\ \nabla_{\hat{B}} \varphi &= 2(-(\tilde{Y}_L + 2\tilde{Z}_L)^* B + (\hat{Y}_L + 2\hat{Z}_L) \hat{B}), \\ \nabla_{\hat{C}} \varphi &= 2(C \tilde{P}_L + \hat{C} \hat{P}_L), \\ \nabla_{\hat{M}_i} \varphi &= 2(-\tilde{P}_L^* M_i \tilde{P}_L + \hat{P}_L^* \hat{M}_i \hat{P}_L), \quad i = 1, \dots, p, \end{aligned}$$

where \tilde{P}_L and \hat{P}_L are the solutions to (5) and (6), respectively. Let $S_L := A^L$ and $\hat{S}_L := \hat{A}^L$. Then $\tilde{Y}_L, \hat{Y}_L, \tilde{Z}_L, \hat{Z}_L$ are the solutions to the finite-horizon Lyapunov/Sylvester equations

$$\tilde{Y}_L = A^* \tilde{Y}_L \hat{A} + C^* \hat{C} - S_L^* C^* \hat{C} \hat{S}_L, \quad (18)$$

$$\hat{Y}_L = \hat{A}^* \hat{Y}_L \hat{A} + \hat{C}^* \hat{C} - \hat{S}_L^* \hat{C}^* \hat{C} \hat{S}_L,$$

$$\tilde{Z}_L = A^* \tilde{Z}_L \hat{A} + \sum_{i=1}^p (M_i \tilde{P}_L \hat{M}_i - S_L^* M_i \tilde{P}_L \hat{M}_i \hat{S}_L), \quad (19)$$

$$\hat{Z}_L = \hat{A}^* \hat{Z}_L \hat{A} + \sum_{i=1}^p (\hat{M}_i \hat{P}_L \hat{M}_i - \hat{S}_L^* \hat{M}_i \hat{P}_L \hat{M}_i \hat{S}_L).$$

Moreover, with $\mathcal{T}_{\hat{A}, L}^*(X) := \sum_{j=0}^{L-1} (\hat{A}^*)^j X (\hat{A}^*)^{L-1-j}$ and

$$\bar{Z}_L = A^* \bar{Z}_L \hat{A} + \sum_{i=1}^p M_i \tilde{P}_L \hat{M}_i, \quad (20)$$

$$\bar{Z}_{r, L} = \hat{A}^* \bar{Z}_{r, L} \hat{A} + \sum_{i=1}^p \hat{M}_i \hat{P}_L \hat{M}_i,$$

$$\tilde{P} = A \tilde{P} \hat{A}^* + B \hat{B}^*, \quad (21)$$

$$\hat{P} = \hat{A} \hat{P} \hat{A}^* + \hat{B} \hat{B}^*,$$

we define

$$V_L := \hat{B}B^*S_L^*\bar{Z}_L - \hat{B}\hat{B}^*\hat{S}_L^*\bar{Z}_{r,L} + \tilde{P}^*S_L^*C^*\hat{C} - \hat{P}\hat{S}_L^*\hat{C}^*\hat{C} + \sum_{i=1}^p (\tilde{P}^*S_L^*M_i\tilde{P}_L\hat{M}_i - \hat{P}\hat{S}_L^*\hat{M}_i\hat{P}_L\hat{M}_i),$$

$$L_L := -(\tilde{Y}_L + \tilde{Z}_L)^*(\tilde{P} - \tilde{P}_L) + (\hat{Y}_L + \hat{Z}_L)(\hat{P} - \hat{P}_L) - (\bar{Z}_L - \tilde{Z}_L)^*\tilde{P}_L + (\bar{Z}_{r,L} - \hat{Z}_L)\hat{P}_L + \mathcal{T}_{\hat{A},L}^*(V_L).$$

Proof. The proof follows from [17]. \square

Theorem 2. Let $\varphi^{(i)}(\hat{\mathcal{S}}^{(i)}) := \|\mathcal{S}^{(i)} - \hat{\mathcal{S}}^{(i)}\|_{h_L^2}^2$ and $K_i := 2\sqrt{\varphi^{(i)}(\hat{\mathcal{S}}^{(i)})}$. Then the gradients of the MOR objective (17) are

$$\begin{aligned} \nabla_{\hat{A}^{(i)}} f &= \frac{\tilde{G}_i}{K_i} \cdot \text{diag}\left(\nabla_{\hat{A}^{(i)}} \varphi^{(i)}\right), \\ \nabla_{\hat{B}^{(i)}} f &= \frac{\tilde{G}_i}{K_i} \cdot \nabla_{\hat{B}^{(i)}} \varphi^{(i)}, \quad \nabla_{\hat{C}^{(i)}} f = \frac{\tilde{G}_i}{K_i} \cdot \nabla_{\hat{C}^{(i)}} \varphi^{(i)}, \\ \nabla_{\hat{M}_j^{(i)}} f &= \frac{\tilde{G}_i}{K_i} \cdot \nabla_{\hat{M}_j^{(i)}} \varphi^{(i)}, \quad j = 1, \dots, m. \end{aligned}$$

Proof. By the chain rule, $df = \sum_i \frac{\tilde{G}_i}{K_i} d\varphi^{(i)} = \sum_i \langle \frac{\tilde{G}_i}{K_i} \nabla_{\theta} \varphi^{(i)}, d\theta \rangle$ with $\theta \in \{\hat{B}^{(i)}, \hat{C}^{(i)}, \hat{M}_j^{(i)}\}$. Moreover, since $\hat{A}^{(i)} = \text{diag}(\hat{\Lambda}^{(i)})$, $d\varphi^{(i)} = \langle \nabla_{\hat{A}^{(i)}} \varphi^{(i)}, d\hat{A}^{(i)} \rangle = \langle \text{diag}(\nabla_{\hat{A}^{(i)}} \varphi^{(i)}), d\hat{\Lambda}^{(i)} \rangle$, which yields the stated expressions. \square

The next lemma is useful when computing the gradient with respect to \hat{U}_j under the constraint $\hat{M}_j = \hat{U}_j^* \hat{U}_j$.

Lemma 4. Let $U \in \mathbb{C}^{c \times n}$, $M = U^*U$, and $f = f(M)$ be a real-valued differentiable function. Then, for the gradient $\nabla_M f$ with respect to M , we have

$$\nabla_U f = U(\nabla_M f + (\nabla_M f)^*).$$

Proof. See Appendix. \square

C. Gradient-Based Algorithm

Algorithm 1 is a stability-guaranteeing gradient-based algorithm derived from Theorem 2. At each iteration, after computing the gradients, backtracking is employed so that the proposed reduced model satisfies the stability constraint and the Armijo condition. Since the A -matrices of the LQO systems (1) considered in this work are diagonal, the gradients can be computed efficiently.

Remark 4. In gradient calculations, it is necessary to compute the large-scale Sylvester equations (18), (19), (20), and (21), and this computation often becomes a computational bottleneck for the algorithm. On the other hand, when the A matrix is diagonal, as in the systems addressed in this study, efficient computation is possible. We consider the discrete-time Sylvester equation

$$\mathcal{X} = \mathcal{A}\mathcal{X}\mathcal{B} + \mathcal{C}, \quad \mathcal{A} \in \mathbb{C}^{n \times n}, \quad \mathcal{B} \in \mathbb{C}^{m \times m}, \quad \mathcal{C} \in \mathbb{C}^{n \times m}.$$

If $\mathcal{A} = \text{diag}(\alpha_1, \dots, \alpha_n)$ and $\mathcal{B} = \text{diag}(\beta_1, \dots, \beta_m)$ are diagonal and $|\alpha_i \beta_j| < 1$ for all i, j , then the solution is available in closed form

$$X_{ij} = \frac{C_{ij}}{1 - \alpha_i \beta_j}, \quad 1 \leq i \leq n, \quad 1 \leq j \leq m,$$

so the system can be solved in $\mathcal{O}(nm)$ time by elementwise operations without resorting to the Bartels-Stewart method [18] which is the famous method for the Lyapunov-type equations.

Theorem 3. Let $\{\hat{\theta}_\ell\}_{\ell \geq 0}$ with $\hat{\theta}_\ell := \{\hat{\Lambda}_\ell^{(i)}, \hat{B}_\ell^{(i)}, \hat{C}_\ell^{(i)}, \hat{U}_\ell^{(i)}\}_{i=1}^\xi$ be the sequence generated by Algorithm 1. Assume that $\{\hat{\theta}_\ell\}$ is bounded and, for every $i \in \{1, \dots, \xi\}$, the limit $\lim_{\ell \rightarrow \infty} \text{diag}(\hat{\Lambda}_\ell^{(i)})$ exists and satisfies stability. Then $\{\hat{\theta}_\ell\}$ converges to a stationary point of problem (17).

Proof. See Appendix. \square

Because the optimization problem (17) is nonconvex, the choice of the initial reduced model is important. As an initial reduced model, one may use the output of existing time-limited MOR methods for LQO systems [17], [19]. Note, however, that the existing time-limited MOR methods [17], [19] do not necessarily guarantee stability of the reduced model.

Algorithm 1 Gradient-based method for (17)

Require: Pretrained Full Order Models
 $\{(\Lambda^{(i)}, B^{(i)}, C^{(i)}, (U_j^{(i)})_{j=1}^m)\}_{i=1}^\xi$, initial ROMs
 $\{(\hat{\Lambda}^{(i)}, \hat{B}^{(i)}, \hat{C}^{(i)}, (\hat{U}_j^{(i)})_{j=1}^m)\}_{i=1}^\xi$, horizon length L ,
steps $\eta_{\text{init}} = (\eta_A, \eta_B, \eta_C, \eta_U)$, Armijo c_1 , backtracking
 ρ , iterations K_{max}

Ensure: $\{(\hat{\Lambda}^{(i)}, \hat{B}^{(i)}, \hat{C}^{(i)}, (\hat{U}_j^{(i)})_{j=1}^m)\}_{i=1}^\xi$

- 1: **for** $\ell = 0, 1, \dots, K_{\text{max}} - 1$ **do**
- 2: Compute objective f_ℓ on $k = 0, \dots, L-1$ and gradients
 $\{(\nabla_{\hat{A}^{(i)}} f_\ell, \nabla_{\hat{B}^{(i)}} f_\ell, \nabla_{\hat{C}^{(i)}} f_\ell, (\nabla_{\hat{U}_j^{(i)}} f_\ell)_{j=1}^m)\}_{i=1}^\xi$.
- 3: Initialize $\eta = (\eta_A, \eta_B, \eta_C, \eta_U) = \eta_{\text{init}}$.
- 4: **while** true **do**
- 5: Propose $\tilde{\Lambda}^{(i)} = \hat{\Lambda}^{(i)} - \eta_A \nabla_{\hat{A}^{(i)}} f_\ell$, $\tilde{B}^{(i)} = \hat{B}^{(i)} - \eta_B \nabla_{\hat{B}^{(i)}} f_\ell$, $\tilde{C}^{(i)} = \hat{C}^{(i)} - \eta_C \nabla_{\hat{C}^{(i)}} f_\ell$, $\tilde{U}_j^{(i)} = \hat{U}_j^{(i)} - \eta_U \nabla_{\hat{U}_j^{(i)}} f_\ell$ for all $i = 1, \dots, \xi$ and $j = 1, \dots, m$.
- 6: **if** any $\text{diag}(\tilde{\Lambda}^{(i)})$ is not stable **then** $\eta_A \leftarrow \rho \eta_A$; **continue**
- 7: Evaluate $f(\tilde{\mathbf{S}})$; set $D_\ell = \eta_A \sum_i \|\nabla_{\hat{A}^{(i)}} f_\ell\|^2 + \eta_B \sum_i \|\nabla_{\hat{B}^{(i)}} f_\ell\|^2 + \eta_C \sum_i \|\nabla_{\hat{C}^{(i)}} f_\ell\|^2 + \eta_U \sum_{i,j} \|\nabla_{\hat{U}_j^{(i)}} f_\ell\|^2$.
- 8: **if** $f(\tilde{\mathbf{S}}) \leq f_\ell - c_1 D_\ell$ **then** accept; **break** **else** $\eta \leftarrow \rho \eta$
- 9: **end while**
- 10: Update $(\tilde{\Lambda}^{(i)}, \tilde{B}^{(i)}, \tilde{C}^{(i)}, (\tilde{U}_j^{(i)})_{j=1}^m) \leftarrow (\hat{\Lambda}^{(i)}, \hat{B}^{(i)}, \hat{C}^{(i)}, (\hat{U}_j^{(i)})_{j=1}^m)$ for $i = 1, \dots, \xi$.
- 11: **end for**

VI. NUMERICAL EXPERIMENTS

In this section, based on the output error bound derived in Section IV and the proposed method described in Sec-

tion V, we construct compressed models for the IMDb task of the Long Range Arena (LRA) dataset [6]. The compression pipeline for Deep SSMs follows the procedure in Section III-B. In particular, unlike existing approaches [11]–[14], we first solve (17) on the pretrained state-space blocks to obtain reduced models that decrease the upper bound on e_ξ defined in (12), and then perform retraining to obtain the final compressed models. The implementation used in this study is based on the code available at <https://github.com/lindermanlab/S5>.

For pretraining, we build a large model using the Deep SSM described in Section III. The main hyperparameters are summarized in Table I, and other hyperparameters are set according to [4]. Furthermore, during training and inference, a linear state-space model discretized by zero-order hold is used. With this configuration, the model has 207,490 trainable parameters, and the accuracy on the IMDb task reached 86.66%.

We next construct reduced models using the existing MOR methods and Algorithm 1. For Algorithm 1, we choose the reduced models obtained by the discretized version of [19, Algorithm 1] or [17, Algorithm 1] as the initial points. For hyperparameters of Algorithm 1, please refer to Table I. As shown in Table I, we compare the following MOR methods: Time-Limited Balanced Truncation (TLBT) [19]; Time-Limited H^2 model reduction (TLH2) [17]; Algorithm 1 initialized by TLBT [19]; Algorithm 1 initialized by TLH2 [17]. Furthermore, we present the results obtained by adopting different values of r at each layer to achieve a smaller objective value for (17). Note that when using TLH2, the initial point employed the output from TLBT rather than a random stable system.

Table I summarizes the objective values of (17) across methods and the compression accuracy with/without retraining. Especially, we report the relative error to the pretrained model after MOR, as well as *TestAcc* for the compressed model before retraining (before) and after retraining (after). Here, *TestAcc* denotes the classification accuracy on the IMDb test dataset; higher is better. Furthermore, all methods in the table use the same number of trainable parameters, 34,114. As noted earlier, the original model has 207,490 trainable parameters; thus, the parameter count is reduced by approximately 80%. r_{list} in the table denotes the per-layer reduced state dimension r . Additionally, HiPPO in the table denotes a model constructed solely with HiPPO initialization [1], i.e., without MOR, for reference. Note that for HiPPO, the relative error for (17) is reported against the pretrained model.

As shown in *TestAcc* (after), MOR-based compression achieves better accuracy than pure HiPPO initialization. Moreover, examining *TestAcc* (after) reveals that for both r_{list} patterns, the proposed h^2 -norm-based optimization method attains superior performance to TLBT and TLH2 while preserving stability. Note that for $r = 32$, TLH2 failed to construct a stability-guaranteed reduced model. Consequently, it cannot be used as an initialization for Algorithm 1, and retraining does not proceed stably in such cases, consistent with the report in [14]. As noted in Remark 2, allocating larger r to shallower layers—thereby reducing the objective (17)—is effective for constructing high-quality compressed models. These results

suggest that designing reduced models with layerwise-varying r that decrease the output error bound derived in Section IV yields accurate compressed models.

For $r_{\text{list}} = [32, 16, 12, 4]$, *TestAcc* (before) values for TLBT and Algorithm 1 initialized with TLBT were 0.8213 and 0.8166, respectively, exceeding the HiPPO model’s post-training accuracy (0.8029). Compared with the original Deep SSM, our method reduces roughly 80% of the trainable parameters with only a 4–5% drop in accuracy. Furthermore, relative to the “Text” results in [13, Fig.2], at a comparable reduced state dimension $r_{\text{list}} = [16] \times 4$, Algorithm 1’s *TestAcc* (before) is superior. These results indicate that a high-accuracy model could be constructed using only MOR, without retraining, enabling low-cost, high-performance deployment in resource-constrained settings.

VII. SUMMARY

In this paper, we derived an output error upper-bound for Deep SSMs that internally contain LQO systems, and presented an optimal h^2 MOR that approximates the final intermediate output. Furthermore, by carrying out MOR so as to reduce the derived output error bound, we demonstrated numerically that accurate compressed models can be constructed.

As future work, we will investigate why high-performance reduced models can be obtained without retraining, as shown in Section VI. In particular, we will examine two points:

- 1) [13] constructs Deep SSMs with sufficiently large n and m , making uncontrollable and unobservable modes less likely, and then performs model reduction guided by the Hankel singular values. With large m , the number of states that can be removed decreases; nevertheless, performance degradation tends to be small.
- 2) Regarding MOR, while we construct reduced models that suppress the error $\|\mathcal{S}^{(i)} - \hat{\mathcal{S}}^{(i)}\|_{h_L^2}$ like [11], [14], our approach is distinguished by performing MOR on LQO systems. MOR incorporating nonlinearity may be effective.

ACKNOWLEDGMENT

This work was supported by JSPS KAKENHI under Grant Numbers 23K28369 and 25KJ0986.

APPENDIX

Proof of Lemma 1. By the triangle inequality, we have

$$\begin{aligned} & \|u_k \otimes u_k - \hat{u}_k \otimes \hat{u}_k\| \\ & \leq \|(u_k - \hat{u}_k) \otimes u_k\| + \|\hat{u}_k \otimes (u_k - \hat{u}_k)\| \\ & = \|u_k - \hat{u}_k\| \|u_k\| + \|\hat{u}_k\| \|u_k - \hat{u}_k\|. \end{aligned}$$

Summing over k and using the Cauchy-Schwarz inequality yields (13). \square

Proof of Lemma 2. Let $P := I - \frac{1}{m}\mathbf{1}\mathbf{1}^\top$, $c := z - \mu\mathbf{1} = Pz$, and $D := \text{diag}(\gamma_1)$. Then, for $\text{LN}_{\gamma_1, \gamma_2}(z) = D\frac{c}{\sigma} + \gamma_2$, its Jacobian is $\nabla_z \text{LN} = D\left(\frac{I}{\sigma} - \frac{cc^\top}{\sigma^3 m}\right)P$. Since $\|P\|_2 = 1$, $\|D\|_2 = \|\gamma_1\|_\infty$, and $\left\|\frac{I}{\sigma} - \frac{cc^\top}{\sigma^3 m}\right\|_2 \leq \frac{1}{\sigma}$ (because $\sigma^2 \geq \varepsilon$),

TABLE I
HYPERPARAMETERS (LEFT) AND COMPRESSED-MODEL PERFORMANCE (RIGHT) ON IMDB. RETRAINING DIFFERS ONLY IN THE STATE DIMENSION: n REPLACES r ; ALL OTHER HYPERPARAMETERS ARE IDENTICAL.

Deep SSM training					
n	m	c	L	ξ	epochs
128	64	1	4096	4	30
Algorithm 1					
K_{\max}	c_1	ρ	η_{init}		
20	$1e-4$	0.5	$(1, 1, 1, 1)$		

Comparison of compressed-model performance across MOR methods			
Method	r_{list}	Relative error for (17)	TestAcc. (before / after)
HiPPO	$[16] \times 4$	1.5050	0.4905 / 0.7907
TLBT	$[16] \times 4$	0.6330	0.7615 / 0.8647
TLH2	$[16] \times 4$	0.6101	0.7642 / 0.8660
Alg. 1 (TLBT init.)	$[16] \times 4$	0.6266	0.7649 / 0.8662
Alg. 1 (TLH2 init.)	$[16] \times 4$	0.6100	0.7640 / 0.8628
HiPPO	$[32, 16, 12, 4]$	1.5729	0.4807 / 0.8029
TLBT	$[32, 16, 12, 4]$	0.3147	0.8213 / 0.8672
Alg. 1 (TLBT init.)	$[32, 16, 12, 4]$	0.3103	0.8166 / 0.8689

it follows for all z that $\|\nabla_z \text{LN}\|_2 \leq \frac{\|\gamma_1\|_\infty}{\sigma} \leq \frac{\|\gamma_1\|_\infty}{\sqrt{\varepsilon}}$, which gives the upper bound.

For the lower bound, at $c = 0$ we have $\sigma = \sqrt{\varepsilon}$ and $\nabla_z \text{LN} = \frac{1}{\sqrt{\varepsilon}} DP$, hence $\text{Lip}(\text{LN}) \geq \frac{1}{\sqrt{\varepsilon}} \max_{\|x\|=1} \|DPx\| \geq \frac{\|\gamma_1\|_\infty}{\sqrt{\varepsilon}} \sqrt{1 - \frac{1}{m}}$. \square

Proof of Lemma 4. Since f is a real-valued differentiable function of $M = U^*U$, we obtain $df = \langle \nabla_M f, dM \rangle$ and $dM = (dU)^*U + U^*dU$. Hence, by properties of the trace and the definition of the inner product,

$$\begin{aligned} df &= \langle \nabla_M f, (dU)^*U \rangle + \langle \nabla_M f, U^*dU \rangle \\ &= \langle U(\nabla_M f)^* + U\nabla_M f, dU \rangle. \end{aligned}$$

Therefore, from $df = \langle \nabla_U f, dU \rangle$ we obtain $\nabla_U f = U(\nabla_M f + (\nabla_M f)^*)$. \square

Proof of Theorem 3. The proof essentially follows from [20, Thm. 2]. By construction, $f : \mathcal{C} \rightarrow \mathbb{R}$ in (17) is smooth. By the boundedness assumption, the closure $K := \{\hat{\theta}_\ell\}$ is compact. Hence, by the extreme value theorem, ∇f is $L_\nabla := \sup_{x \in K} \|\nabla^2 f(x)\| < \infty$ -Lipschitz on K .

For $s_\ell := \hat{\theta}_{\ell+1} - \hat{\theta}_\ell$, we have $\|s_\ell\|^2 = \eta_\Lambda^2 \|\nabla_{\hat{\Lambda}} f\|^2 + \eta_B^2 \|\nabla_{\hat{B}} f\|^2 + \eta_C^2 \|\nabla_{\hat{C}} f\|^2 + \eta_U^2 \|\nabla_{\hat{U}} f\|^2 \leq \eta_{\text{init}} D_\ell$, and

$$f(\hat{\theta}_{\ell+1}) \leq f(\hat{\theta}_\ell) - \frac{c_1}{\eta_{\text{init}}} \|s_\ell\|^2. \quad (22)$$

Since f is bounded below on K , summing (22) shows $\sum_{\ell=0}^{\infty} \|s_\ell\|^2 < \infty$, hence $\|s_\ell\| \rightarrow 0$.

Because the iterates remain at a positive distance from the instability boundary, there exists $\underline{\eta} > 0$ with $\eta_\Lambda \geq \underline{\eta}$ for all accepted steps. From $\eta_\Lambda \leq \min\{\eta_B, \eta_C, \eta_U\}$, we get $\|\nabla f(\hat{\theta}_{\ell+1})\| \leq (L_\nabla + \underline{\eta}^{-1}) \|s_\ell\|$.

For the rest, using the same proof as in [20, Thm. 2] and the result in [21, Thm. 3.2], we can see that Algorithm 1 converges to a stationary point in K . \square

REFERENCES

- [1] A. Gu, T. Dao, S. Ermon, A. Rudra, and C. Ré, “Hippo: Recurrent memory with optimal polynomial projections,” in *Advances in Neural Information Processing Systems*, 2020, pp. 1474–1487.
- [2] A. Gu, I. Johnson, K. Goel, K. Saab, T. Dao, A. Rudra, and C. Ré, “Combining Recurrent, Convolutional, and Continuous-time Models with Linear State-Space Layers,” in *Advances in Neural Information Processing Systems*, vol. 34, 2021.
- [3] A. Gu, K. Goel, and C. Ré, “Efficiently modeling long sequences with structured state spaces,” in *International Conference on Learning Representations*, 2022.
- [4] J. T. Smith, A. Warrington, and S. Linderman, “Simplified State Space Layers for Sequence Modeling,” in *International Conference on Learning Representations*, 2023.
- [5] A. Gu and T. Dao, “Mamba: Linear-time sequence modeling with selective state spaces,” *arXiv preprint arXiv:2312.00752*, 2023.
- [6] Y. Tay, M. Dehghani, S. Abnar, Y. Shen, D. Bahri, P. Pham, J. Rao, L. Yang, S. Ruder, and D. Metzler, “Long range arena: A benchmark for efficient transformers,” in *International Conference on Learning Representations*, 2021.
- [7] A. Vaswani, N. Shazeer, N. Parmar, J. Uszkoreit, L. Jones, A. N. Gomez, L. Kaiser, and I. Polosukhin, “Attention is all you need,” in *Advances in Neural Information Processing Systems*, vol. 30, 2017.
- [8] X. Wang, S. Wang, Y. Ding, Y. Li, W. Wu, Y. Rong, W. Kong, J. Huang, S. Li, H. Yang *et al.*, “State space model for new-generation network alternative to transformers: A survey,” *arXiv preprint arXiv:2404.09516*, 2024.
- [9] N. Nishikawa and T. Suzuki, “State Space Models are Provably Comparable to Transformers in Dynamic Token Selection,” in *The Thirteenth International Conference on Learning Representations*, 2025. [Online]. Available: <https://openreview.net/forum?id=QFgbJOYJSE>
- [10] Y. Cheng, D. Wang, P. Zhou, and T. Zhang, “Model compression and acceleration for deep neural networks: The principles, progress, and challenges,” *IEEE Signal Processing Magazine*, vol. 35, no. 1, pp. 126–136, 2018.
- [11] H. Ezoe and K. Sato, “Model Compression Method for S4 with Diagonal State Space Layers using Balanced Truncation,” *IEEE Access*, 2024.
- [12] M. Forgione, M. Mejari, and D. Piga, “Model order reduction of deep structured state-space models: A system-theoretic approach,” *arXiv preprint arXiv:2403.14833*, 2024.
- [13] M. Gwak, S. Moon, J. Ko, and P. Park, “Layer-Adaptive State Pruning for Deep State Space Models,” in *Advances in Neural Information Processing Systems*, vol. 37, 2024, pp. 10613–10645.
- [14] H. Sakamoto and K. Sato, “Compression Method for Deep Diagonal State Space Model Based on \mathcal{H}^2 Optimal Reduction,” *IEEE Control Systems Letters*, 2025.
- [15] P. Benner, P. Goyal, and I. P. Duff, “Gramians, energy functionals, and balanced truncation for linear dynamical systems with quadratic outputs,” *IEEE Transactions on Automatic Control*, vol. 67, no. 2, pp. 886–893, 2021.
- [16] S. Reiter, I. Pontes Duff, I. V. Gosea, and S. Gugercin, “ \mathcal{H}_2 optimal model reduction of linear systems with multiple quadratic outputs,” *arXiv preprint arXiv:2405.05951*, 2024.
- [17] U. Zulfiqar, Z.-H. Xiao, Q.-Y. Song, M. M. Uddin, and V. Sreeram, “Time-limited \mathcal{H}_2 -optimal model order reduction of linear systems with quadratic outputs,” *arXiv preprint arXiv:2408.05965*, 2024.
- [18] R. H. Bartels and G. W. Stewart, “Solution of the matrix equation $AX + XB = C$,” *Communications of the ACM*, vol. 15, no. 9, pp. 820–826, 1972.
- [19] Q.-Y. Song, U. Zulfiqar, Z.-H. Xiao, M. M. Uddin, and V. Sreeram, “Balanced truncation of linear systems with quadratic outputs in limited time and frequency intervals,” *arXiv preprint arXiv:2402.11445*, 2024.
- [20] H. Sakamoto and K. Sato, “Data-driven h^2 model reduction for linear discrete-time systems,” *arXiv preprint arXiv:2401.05774*, 2025.
- [21] H. Attouch, J. Bolte, and B. F. Svaiter, “Convergence of descent methods for semi-algebraic and tame problems: proximal algorithms, forward–backward splitting, and regularized Gauss–Seidel methods,” *Mathematical programming*, vol. 137, no. 1, pp. 91–129, 2013.